

Creating two-qudit maximally entangled quantum link through bulk

Keshav Das Agarwal¹, Sudip Kumar Halder^{1,2}, Aditi Sen(De)¹

¹Harish-Chandra Research Institute, A CI of Homi Bhabha National Institute,
Chhatnag Road, Jhansi, Allahabad - 211019, India and

²Department of Physics and Material Science & Engineering,
Jaypee Institute of Information Technology, Noida - 201304, India

We design a set-up for creating maximally entangled two-qudit links between distant nodes which are weakly coupled with interacting spin- s bulk (processor). We exhibit that such quantum links of arbitrary spin quantum number can be formed when the system is prepared at a very low temperature. We find that the Heisenberg and the bilinear-biquadratic (BBQ) spin- s models are the potential candidates to achieve the maximal entanglement in equilibrium. By eliminating the equilibrium requirement, we show that a completely polarized state in the bulk and a suitable qudit state in the link can evolve over time to produce a highly entangled state, as per the BBQ Hamiltonian with nearest- and next-nearest neighbor interactions. When the number of sites in the bulk grows, so does the maximum entanglement produced in dynamics. Further, both the static and the dynamical protocols presented here remain efficient even if the spin quantum numbers of the bulk and the connection are unequal.

I. INTRODUCTION

Entanglement [1], a purely quantum concept originally introduced by Schrödinger [2], is the key resource for developing quantum technologies such as quantum communication and quantum computation [3]. Entangled photons are widely used in quantum communication due to their weakly interacting nature, which is important in preventing decoherence, and also taking advantage of the already available optical fiber technology [4]. Transmitting information across distant physical qubits is still challenging [5–7]. Additionally, short-range quantum communication is increasingly gaining importance in quantum computation as it is required to connect different quantum processors to build a powerful quantum computer [8–10] and hence exploring ways to link processors into a modular system is an important avenue of research. This raises an interesting problem in the world of quantum computing since such a connection between processors involves the generation of a highly entangled state later employed for state transfer protocol.

In this context, spin chains emerge as an acceptable alternative to photons for establishing entangled quantum links (EQL) (also referred to as long-distance entanglement (LDE)) between processors (bulk), at least, for short- and mid-range communication [11, 12]. More specifically, it is demonstrated that two spin-1/2 systems, called A and B , separated by some distance can share a maximally entangled state when they interact via a spin chain that includes only nearest-neighbor and next-nearest neighbor interactions, creating a resourceful quantum link [12–18]. Note that monogamy of entanglement [19] demands that the interaction between A (and B) and the spins of the bulk be weaker than the typical interaction between the spins contained in the bulk [12]. Further, antiferromagnetic spin systems [20], such as antiferromagnetic XXZ spin chain with alternating interactions [21], and other variations of Heisenberg spin-1/2 chain [22], Heisenberg spin-1 chain [23] with bilinear-biquadratic interaction [12, 24], are examples of strongly correlated systems that normally make up the bulk. However, such systems usually have energy gaps above the ground state that vanish exponentially with the

increase of the length of the spin chain[12]. This suggests that EQL can only be established at absolute zero temperature which is physically untenable. Alternatively, the ground state of certain spin chains like the open XX model with weak “end bond” interactions can have a kind of long-distance entanglement, referred to as “quasi-long-distance” entanglement, between the end spins of the chain which decays very slowly with the length of the chain [14] since the energy gap of these systems vanishes algebraically with the size of the system. As a result, quasi-long-distance entanglement is less susceptible to thermal excitations and may be better suited for short-range quantum communication. Entanglement between two spins approximately $220 - 250\text{\AA}$ apart has been created through a spin chain prepared from $\text{Sr}_{14}\text{Cu}_{24}\text{O}_{41}$ block materials below 2.1K in laboratories [25]. In a similar spirit, a nitrogen-vacancy (NV) center-based link connected by a quantum channel was proposed [16] (see also [26]). However, the majority of the studies in this direction describe how to prepare a two-qubit maximally or highly entangled quantum connection in equilibrium. We depart from both the equilibrium situation and the dimensional constraint in this study.

Higher-dimensional quantum systems have more resources [27–29], making them more useful in variety of quantum information processing tasks including quantum cryptography [30–32], quantum computation [33], quantum thermal devices [34–39] compared to qubit-based systems. Further, such systems have also been prepared in laboratories to demonstrate dimensional advantages in quantum protocols by using several physical substrates including photons [40–45], trapped ions[46], NV centre [47], superconducting circuits [48] and so on. One intriguing question to consider is: “*Is it possible to create a two-qudit entangled quantum link between distant sites using bulk made up of multiple interacting spins?*” This is especially relevant if quantum processors are constructed with qudit or qubit states. We first answer this question affirmatively. This raises an immediate question: *Is it necessary to accomplish this by having the bulk and quantum link’s spin quantum numbers equal?* We determine that this is not necessary to establish a maximally or highly entangled quantum link. In particular, we report that the maximally entangled

two-qudit state can be established at near zero temperature when we take a spin-1/2 interacting bulk system following Heisenberg interactions and the link as spin- s which is weakly coupled to the bulk. However, when the bulk is replaced by spin-1 bilinear-biquadratic Hamiltonian [24, 49–53] and the link follows the same interactions although weak, the maximal entanglement can be obtained with a greater control of the system in comparison with the spin-1/2 bulk state by suitably adjusting the system parameters. Up to a moderate system size, all of the results reported here are system-independent.

We exhibit that by initializing the bulk state in a totally polarized (product) state and the link in a different rotated product state, we may construct a highly entangled state in the link using the same Hamiltonian as used in the equilibrium study. For both equilibrium and dynamical investigations, we observe that next-nearest-neighbor interactions have no effect on entanglement. In contrast to thermal state analysis, entanglement of the dynamical state is dependent upon the bulk system-size, which rises as the number of sites grows.

The organization of this paper is as follows. In Sec. II, we describe the framework for creating entangled quantum links both in equilibrium and non-equilibrium scenarios and also discuss how to handle this problem using numerical methods since the model considered here cannot be solved analytically. The model considered in this work is introduced in Sec. III A. The set-up of obtaining a maximally entangled state between two distant sites in the equilibrium case is presented in Sec. III B when the bulk consists of spin-1/2 and in Sec. III C for spin-1 bulk state. Sec. IV reports how to create a highly entangled quantum link between two distant nodes dynamically. The results are summarized in Sec. V.

II. FRAMEWORK OF BUILDING ENTANGLED LINKS

Let us describe the set-up in which the entangled quantum link can be established. Suppose that there is a bulk (processor), C , consisting of interacting spins with spin quantum number s_b , forming a lattice structure while there are two distant spin- s_ℓ systems, denoted as A and B , weakly coupled with the bulk (as shown in Fig. 1). Our aim is to find the optimum equilibrium conditions to have maximum entanglement between A and B of a given dimension ($d_\ell = 2s_\ell + 1$) by tuning the interactions of the bulk and the link. Such a scenario is considered before in literature when $s_b = 1/2$ and $s_\ell = 1/2$ or both of them are spin-1 systems [12–18]. It is intriguing to find the strength of interactions and other system parameters responsible for achieving maximal entanglement between quantum links when $s_\ell \geq s_b$ for different values of s_ℓ and s_b . It is plausible to assume that to obtain a maximally entangled link, we require $s_\ell = s_b$ or $s_\ell < s_b$ which we will show not to be the case. Moreover, all the studies in literature have presented a preparation procedure of entangled states at zero-temperature. Going beyond that, we examine how to create maximum entanglement between link spins over time, starting from a suitable initial state. In this situation, we identify the appropriate initial state, time, and system parameters that are required to produce highly entangled links having no di-

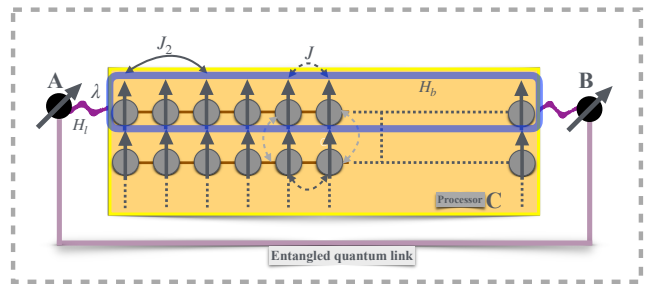


FIG. 1. Schematic diagram of a quantum processor which is attached to two distant sites, referred to as a quantum link. Quantum processor (bulk) consists of several spin- s systems which interact according to some interacting Hamiltonian, H_b . The link sites interact with the bulk weakly, dictated by H_ℓ where we assume that the couplings between the sites in the bulk, $\{J, J_2\}$ is much stronger than the interactions between the link and the edge sites of the bulk, λ . The goal is to create a highly entangled quantum link (EQL) situated in distant locations both at zero- and non-zero temperatures and through evolution. In our study, we assume that the bulk is a spin chain with open boundary condition and hence the other arrays of spins in the processor is weakly coupled with the one-dimensional array (the blue box). We demonstrate that it is indeed possible to produce a highly EQL by appropriately adjusting the interactions in equilibrium and the evolving Hamiltonian as well as the initial states in the non-equilibrium case.

rect interactions between them. The scaling analysis is also performed in both static and dynamical situations.

A. Quantifying entanglement between two link spins

Entangled state in equilibrium scenario. We are interested in quantifying the quantum resource content of the link sites, A and B . To do so, the N -party thermal state at temperature T of the combined system, $\rho_{ABC} \propto \exp(-\beta H^{(s_\ell, s_b)}(\lambda))$ with $\beta = \frac{J}{k_B T}$ (k_B being the Boltzmann constant) is prepared, where λ is interaction strength between a link sites and a corresponding edge site of the bulk. Setting β very large, we compute two-party reduced density matrix in the $\mathbb{C}^{d_\ell} \otimes \mathbb{C}^{d_\ell}$ Hilbert space with d_ℓ being the individual dimension of the link site after tracing out $(N - 2)$ party of the bulk.

Logarithmic negativity – an entanglement measure. The entanglement is quantified by logarithmic negativity (LN) [54]. It is defined as $\mathcal{E} = \log_2(2\mathcal{N}(\rho_{AB}) + 1)$ for the bipartite state ρ_{AB} . Here $\mathcal{N}(\rho_{AB})$ is its negativity which is the absolute sum of the negative eigenvalues of the partially transposed state $\rho_{AB}^{T_A}$ (or $\rho_{AB}^{T_B}$) with the transpose being taken either over the party A (or B) [55, 56]. While $\mathcal{E} = 0$ is only a necessary condition of separability for $d_A d_B > 6$ with d_A , and d_B being the dimension of A and B respectively [57–59], it is also a sufficient condition for a large class of $SU(2)$ symmetric states [60]. Nonetheless, a non-zero \mathcal{E} confirms that the state ρ_{AB} is entangled. Therefore, LN is maximum ($\log_2 d_\ell$) for

$\rho_{AB} = |\Phi_{AB}^+\rangle\langle\Phi_{AB}^+|$ ($|\Phi_{AB}^+\rangle = \frac{1}{\sqrt{d_\ell}} \sum_{k=-s_\ell}^{s_\ell} |kk\rangle$) and its local unitarily equivalent state. To perform a fair comparison, we scale $\tilde{\mathcal{E}}$ of the bipartite state ρ_{AB} of the link sites having individual dimension d_ℓ as $\mathcal{E} = \frac{1}{\log_2 d_\ell} \tilde{\mathcal{E}}$.

Dynamical state. Instead of a thermal state, we start with a product state, $|\Psi(t=0)\rangle = |\psi_b\rangle^{\otimes(N-2)} |\psi_\ell\rangle^{\otimes 2}$ and evolve it with the Hamiltonian $H^{(s_\ell, s_b)}(\lambda)$. The dynamical N -party state becomes $|\Psi(\lambda, t)\rangle$. The maximal entanglement created in the bipartite reduced density matrix of the links A and B , $\rho_\ell(\lambda, t)$ obtained from $|\Psi(\lambda, t)\rangle$ is the main concern of this work, where the maximization is performed over time, i.e., $\mathcal{E}^{\max}(\rho_\ell(\lambda, t)) = \max_{t, \lambda, \dots} \mathcal{E}(\rho_\ell)$ where maximization is performed over all the system parameters like t, λ . Further, we are also interested in studying the trends of average entanglement created in this process, $\langle \mathcal{E} \rangle = \sum_t \mathcal{E}(\rho_\ell)$ where the averaging is performed over a large time till the convergence of $\langle \mathcal{E} \rangle$ is achieved.

Numerical simulation technique. Since we will be dealing with higher dimensional systems and the role of next-nearest neighbor (NNN) interactions along with nearest-neighbor (NN) ones, the spin models both in equilibrium and non-equilibrium situations cannot be solved analytically and hence the entire analysis has to be carried out by numerical methods. Let us briefly discuss how we perform the numerical simulation.

To compute LN, we use the exact diagonalization procedure based on the Lanczos method [61–63] to find the low-lying states of the model. In the extreme case, i.e., if $\lambda \rightarrow 0$, the ground state degeneracy is $\sim d_\ell^2$, along with approximate degeneracies (if any) in the finite-size bulk Hamiltonian, we compute $3d_\ell^2$ low-lying eigenstates and take the thermal average of them while ensuring that $e^{-\beta\Delta E_{\max}} < \epsilon$, where ΔE_{\max} is the difference between the maximum eigenenergy and the minimum one and $\epsilon \sim O(10^{-6})$. This ensures that all the relevant states that can contribute to the calculation of entanglement are considered for each β . We also compute the purity of the thermal state as $\mathcal{P} = \frac{1}{Z} \sum_k (e^{-\beta E_k})^2$, with $Z = \sum_k e^{-\beta E_k}$ being the partition function, and summation is taken over all the lowest eigenvalues computed. $\mathcal{P} \in (0, 1]$ and denoting E_{gap} as the energy difference between the two lowest energy eigenvalues, \mathcal{P} is close to 1 when $\beta E_{gap} \gg 1$, i.e., when the ground state is non-degenerate and the temperature is low enough in the energy scale, so that the unique ground state is achieved.

In the dynamical scenario, we look at the entanglement generation capability of the model which is quantified from the entanglement of an evolved state $|\Psi(\lambda, t)\rangle = e^{-iH(\lambda)t} |\Psi_0\rangle$ via unitary evolution from a product initial state, $|\Psi(t=0)\rangle$. We compute the reduced density matrix ρ_{AB} of N -party dynamical state, $\rho(\lambda, t) = |\Psi(\lambda, t)\rangle\langle\Psi(\lambda, t)|$. To handle the situation numerically, we apply the Chebyshev series approximation to the unitary operator [64, 65], where only a finite term of the series are taken. This technique is efficient as it only requires the action of the Hamiltonian on an arbitrary state and as the number of the terms in the series increases linearly with the increase of the dimension of the Hilbert space in the evolved state and the time step of the evolution.

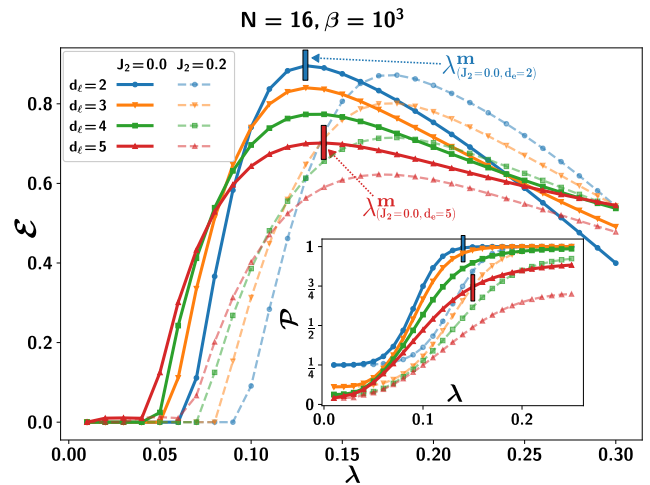


FIG. 2. **Entanglement of a quantum link, \mathcal{E} for different individual dimensions of the link site, d_ℓ .** \mathcal{E} (ordinate) against the interaction strength λ (abscissa) between the link and the bulk sites for different dimensions d_ℓ of the link node, with and without next-nearest interaction strength J_2 . The bulk consists of spin-1/2 systems and the entire system (bulk + link) is prepared in a thermal state with $\beta = 10^3$. We observe that the maximum entanglement achieved at λ^m decreases with the increase of d_ℓ . (Inset) Purity \mathcal{P} for the corresponding system with λ having vertical bars at λ^m where the maximum entanglement, \mathcal{E}^{\max} is achieved. The total system-size including two link sites is taken to be 16. All quantities are dimensionless.

III. TWO-QUDIT ENTANGLED QUANTUM LINKS THROUGH BULK SPIN- s CHAIN IN EQUILIBRIUM-DIMENSIONAL BENEFIT

We now explore the creation of a maximally entangled quantum link by adjusting system parameters at near-zero temperatures. The system considered contains the bulk consisting of interacting spin-1/2 or spin-1 chains and the two link sites with varying spin- s_ℓ systems which are weakly connected with the bulk. First, we describe the Hamiltonian and the motivation to examine it, which is followed by the results obtained in this set-up.

A. Set the stage - Hamiltonian for the bulk and the quantum link

Before describing the system with non-identical bulk and link spins, let us consider the model with identical spin-1/2 bulk and link spin systems. It was shown that when the Hamiltonian of the bulk is the nearest-neighbor XX chain and the quantum links follow the nearest-neighbor XY interactions with the edge spins of the bulk [18], quantum links can share maximal entanglement by suitably tuning system parameters. Specifically, $H_b = \sum_{i=2}^{N-2} \hat{S}_i^x \hat{S}_{i+1}^x + \hat{S}_i^y \hat{S}_{i+1}^y$ and $H_\ell = \lambda_1 (\hat{S}_1^x \hat{S}_2^x + \hat{S}_{N-1}^x \hat{S}_N^x) + \lambda_2 (\hat{S}_1^y \hat{S}_2^y + \hat{S}_{N-1}^y \hat{S}_N^y)$, where \hat{S}_i^α , ($\alpha = x, y$) are spin-1/2 operators at i -th site, H_b describes the bulk Hamiltonian and H_ℓ is the Hamiltonian

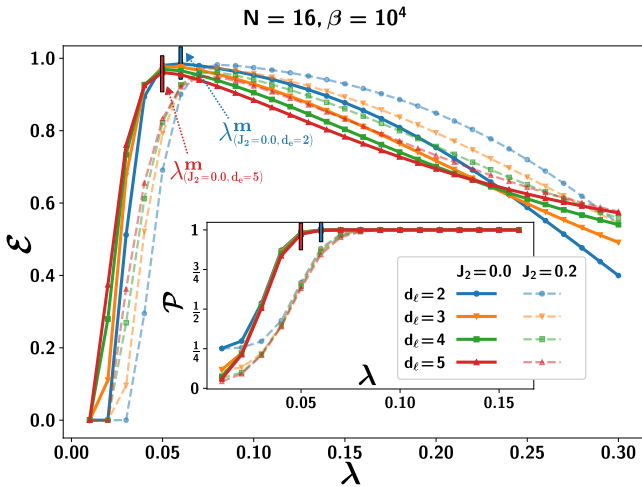


FIG. 3. \mathcal{E} (ordinate) of the link vs λ (abscissa) for different link spin dimension d_ℓ . Here $\beta = 10^4$. All other specifications are same as in Fig. 2. Notice here that for low temperature, maximally entangled quantum links can be established for all the dimension at certain λ values, denoted as λ^m even with a spin-1/2 bulk system. All quantities are dimensionless.

connecting the link to the bulk. Hence, the total Hamiltonian of the system can be represented as $H^{(\frac{1}{2}, \frac{1}{2})}(\lambda, \gamma) = H_b^{\frac{1}{2}} + \lambda H_\ell^{(\frac{1}{2}, \frac{1}{2})}(\gamma)$ ($\lambda = \frac{\lambda_1 + \lambda_2}{2}, \gamma = \frac{\lambda_1 - \lambda_2}{\lambda_1 + \lambda_2}$), with γ as the anisotropy parameter of the connecting Hamiltonian described by the XY model and the superscript ($s_\ell = 1/2, s_b = 1/2$) represents the spin quantum numbers of the link, s_ℓ , and the bulk, s_b . Let us now keep the bulk Hamiltonian to be spin-1/2 systems while the link spins among which the production of maximal entanglement is desirable, are taken to be spin-1. It implies that edge spins of the bulk with which link sites interact remain spin-1/2 so that the total Hamiltonian, $H_\ell^{(1, \frac{1}{2})}$, becomes the mixed spin Hamiltonian following XY interactions. It is important to note here that when $\lambda < 1$, we find that no tailoring of interactions leads to a maximum entanglement between A and B . This suggests that only changing the spin-1/2 quantum links to a spin-1 one may not work.

To resolve the situation, we adopt the Heisenberg Hamiltonian having the nearest- and the next-nearest neighbor interactions. Specifically, we consider Heisenberg interaction for $s_b = \frac{1}{2}$ chain with different s_ℓ at the links A and B . For $s_b = 1$ chain, the inter-spin interactions are taken to be bilinear-biquadratic (BBQ) [24, 49–53]. The coupling between the spins $s_b = 1$ of C and the spins s_ℓ at A and B are also taken as bilinear-biquadratic with different interaction strength than the bulk except for $s_\ell = \frac{1}{2}$. For spin $s_\ell = \frac{1}{2}$, the coupling between A (or B) and C is taken as Heisenberg type.

More specifically, we have

$$H^{(s_\ell, s_b)}(\lambda) = JH_b^{s_b} + \tilde{\lambda}H_\ell^{(s_\ell, s_b)}, \quad (1)$$

$$H_b^{(s_\ell, s_b)} = \sum_{i=2}^{N-2} H_{i, i+1} + J_2 \sum_{i=2}^{N-3} H_{i, i+2}, \quad (2)$$

$$H_\ell^{s_b} = H_{1,2} + H_{N-1,N} + J_2(H_{1,3} + H_{N-2,N}), \quad (3)$$

$$H_{i,j} = \begin{cases} \vec{S}_i \cdot \vec{S}_j & \text{if } i \text{ or } j \text{ is spin-1/2} \\ \cos \theta \vec{S}_i \cdot \vec{S}_j + \sin \theta (\vec{S}_i \cdot \vec{S}_j)^2 & \text{otherwise} \end{cases}, \quad (4)$$

where $\vec{S}_i = \hat{S}_i^x \hat{x} + \hat{S}_i^y \hat{y} + \hat{S}_i^z \hat{z}$ is an arbitrary spin operator in a three-dimensional space acting at the i th site and note that the two-body Hamiltonian, $H_{i,j}$ is $SU(2)$ invariant. We study the antiferromagnetic interactions, i.e., $J > 0$, the dimensionless parameter $\lambda = \frac{\tilde{\lambda}}{J}$ gives the relative coupling strength between A (or B) and the bulk, and J_2 is the strength of next-nearest neighbor interaction, both relative to the nearest-neighbor strength J . Note further that when either of the i -th or j -th site is a spin-1/2 system, $(\vec{S}_i \cdot \vec{S}_j)^2 = \frac{1}{2}(\mathbb{I} - \vec{S}_i \cdot \vec{S}_j)$. Therefore, in such cases, there is no bi-quadratic term and the Hamiltonian reduces to the Heisenberg-like model. We look into the equilibrium properties of the system, namely quantum entanglement between the two link sites in the thermal state of the system at a very low temperatures which is also termed as the long-distance entanglement (LDE) [12, 18]. As reaching ground states require extremely low temperature and long equilibration time, we also look into the dynamical scenario, where the system, initially in a product state, is evolved under the $SU(2)$ Hamiltonian. We study its capability of entangling the initially separable links via unitary evolution.

B. Spin- $\frac{1}{2}$ bulk vs spin- s_ℓ quantum link

Let us first study the system with spin-1/2 in the bulk C and vary link spins s_ℓ at A and B . This investigation deals with the scenario when $s_b \leq s_\ell$. We find that the antiferromagnetic Heisenberg interactions can maximally entangle the link spins A and B irrespective of the value of s_ℓ . For a very small coupling, i.e., when $\lambda < \lambda^v$ with λ^v being the link-strength corresponding to a vanishing entanglement between the links, we notice that at a high inverse temperature β , the number of closely spaced low-lying states $\propto d_\ell^2$ reduces the purity \mathcal{P} of the thermal state $\rho(\beta, \lambda)$, resulting to the reduction of the entanglement between A and B . For example, at $\beta = 10^3$, the purity \mathcal{P} is $\frac{1}{4}$ for $d_\ell = 2$, which, in turn, possesses a vanishing entanglement between the two-qubit link state (see Fig. 2). Further, we notice that the link interaction strength, λ^v , required to have non-vanishing entanglement decreases with the increase of dimensions d_ℓ of the individual site of the link. As λ is increased, initially \mathcal{P} increases very slowly with practically no gain in entanglement although, with moderate values of λ , \mathcal{P} starts increasing faster with λ and \mathcal{E} also starts growing. \mathcal{E} reaches a maximum, denoted as \mathcal{E}^{\max} at $\lambda^m = \max_\lambda \mathcal{E}$. Three immediate observations emerge -

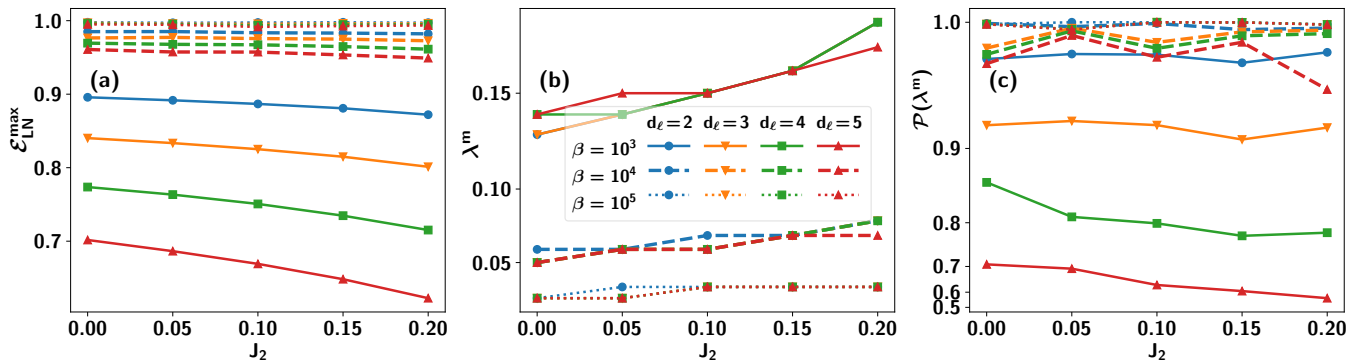


FIG. 4. Establishing entangled quantum link with the variation of NNN interaction strength J_2 (abscissa) in spin-1/2 bulk ($s_b = 1/2$). (a) \mathcal{E}_{LN}^{\max} (ordinate) represents the maximum entanglement that can be prepared between the link site and the edge of the bulk. (b) Edge interaction strength λ^m (ordinate) where \mathcal{E}^{\max} is achieved against J_2 . (c) Purity $\mathcal{P}(\lambda^m)$ (ordinate) at the edge interaction strength λ^m with J_2 . Solid, dashed and dotted lines represent different inverse temperature values, $\beta = 10^3$, $\beta = 10^4$ and $\beta = 10^5$ respectively. Circle, inverted triangle, square and triangle are for different dimensions of the link sites, namely, $d_\ell = 2, 3, 4,$ and 5 respectively. The system-size is $N = 16$. All quantities are dimensionless.

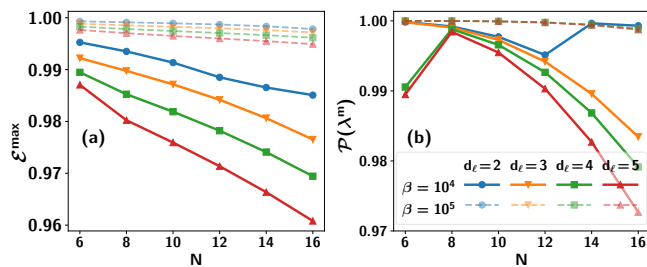


FIG. 5. **Finite-size effects on EQL.** (a) \mathcal{E}^{\max} (ordinate) against system-size N (abscissa) and (b) Purity $\mathcal{P}(\lambda^m)$ at λ^m (ordinate) vs N . Here $J_2 = 0.0$. It is evident that with the increase of β , \mathcal{E}^{\max} does not depend on the system-size. All other specifications are same as in Fig. 4. All quantities are dimensionless.

(i) \mathcal{E} decreases with the increase of d_ℓ for $\beta = 10^3$ which does not change substantially when β is further increased to 10^4 (comparing Figs. 2 and 3); (ii) the behavior of \mathcal{E}^{\max} is directly connected to the purity of the entire state; (iii) λ^m almost remains constant with d_ℓ as also shown in Fig. 4. All the observations depend on the temperature chosen. Specifically, very low temperatures can erase any differences seen due to the increase of individual dimension of the link node. We also notice that \mathcal{E} decreases further with the increase of λ since the monogamy property of entanglement [19] prevents a large entanglement between two sites at A and B in the presence of strong coupling with spins s_b of the C . Therefore, there is a trade-off between coupling strength λ and inverse temperature β to achieve high entanglement \mathcal{E}^{\max} between the two link spins. Lowering the temperature to $\beta = 10^4$, $\mathcal{E}^{\max} \sim 1$ is achieved for all link spins (Fig. 3), with $\mathcal{P}(\lambda^m) \sim 1$ even at small λ as lower energy window can be accessed.

Role of next-nearest neighbor interactions. It is believed that with the increase in the range of interactions, entanglement can be distributed among more sites in the spin chain [66–69]. However, the goal of this work is to maximize entanglement between the links which possibly implies

disentangling the $AB : C$ bipartition from the monogamy of entanglement. Therefore, in this situation, it is not obvious to see whether the next-nearest neighbor interactions along with nearest-neighbor interactions helps in achieving the goal. We observe that in the presence of the NNN interaction, $\mathcal{P}(\lambda^m) \sim 1$ for higher λ and, therefore, \mathcal{E} achieves its maximum at a higher λ^m although the peak value \mathcal{E}^{\max} itself reduces slightly (see Fig. 4). These effects of NNN become more pronounced at lower β as shown in Fig. 4. This is again due to the monogamy of entanglement since with the increase of entanglement shared among many parties, entanglement between link pairs declines.

Let us summarise the observations in this case when $s_b = \frac{1}{2}$ and s_ℓ is arbitrary - (i) \mathcal{E}^{\max} remains almost constant with the increase of the strength of NNN (upto a moderate J_2) at λ^m ; (ii) λ^m also does not change substantially with $J_2 \leq 0.2$; (iii) $\mathcal{P}(\lambda^m) \sim 1$ for $J_2 \leq 0.2$; (iv) all the results hold for substantially low temperature, i.e., with high β . Otherwise, J_2 -dependence of \mathcal{E}^{\max} , λ^m and \mathcal{E}^{\max} is prominent for high β values (see Fig. 4 with $\beta \leq 10^3$).

Finite-size scaling. It is important to determine whether the results presented above remain valid with the increase in system-size of the bulk C or not. Again, we observe that entanglement, as well as purity, remains unaltered with the increase of N provided the temperature is very low, i.e., $\beta \sim \mathcal{O}(10^4)$ or so.

The antiferromagnetic Heisenberg model is known to host gapless excitation in the thermodynamic limit, and hence the entanglement between two spin- $\frac{1}{2}$ sites, A and B is expected to decay with the increase in system-size N except at zero temperature [70]. The behavior of \mathcal{E}^{\max} with the system-size N of the entire system by varying s_ℓ at A and B is depicted in Fig. 5. We find that the decay of \mathcal{E}^{\max} with N is increasing with the increase of s_ℓ , especially for moderate $\beta = 10^3$. This shows that the physically untenable requirement of extremely low temperature (close to absolute zero) for achieving two-qubit maximal entanglement [14, 18] through a macroscopic spin- $\frac{1}{2}$ chain cannot be avoided by using qudits in the quantum

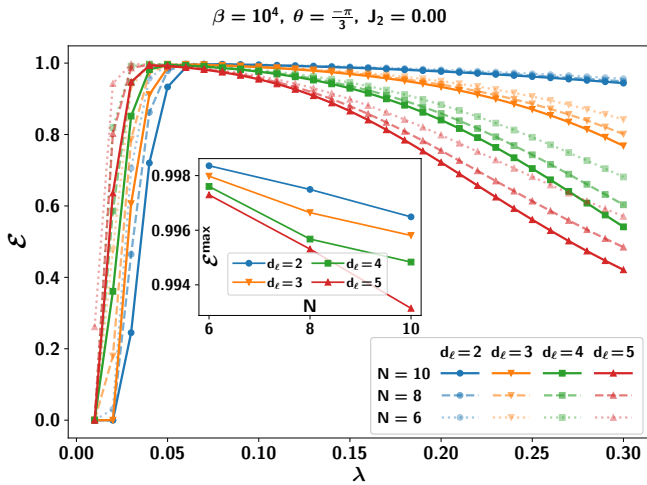


FIG. 6. Two-qudit entangled link, \mathcal{E} (ordinate), against coupling constant λ (abscissa) through a spin-1 bulk having only nearest-neighbor interaction (i.e., $J_2 = 0$). All the spins including the link sites interact according to the bilinear-biquadratic Hamiltonian with $\theta = -\frac{\pi}{3}$. The thermal state is prepared at $\beta = 10^4$. Solid, dashed and dotted line represent $N = 10, 8$ and 6 for different individual dimension of the link d_ℓ at A and B . The effects of system-size N (abscissa) on \mathcal{E}^{\max} (ordinate) is shown in the inset. All quantities are dimensionless.

links.

C. Entangled link through bulk spin-1 chain

First, we assume that there is only nearest-neighbor interaction among spins $s_b = 1$ in C and the link spins s_ℓ at A and B interact only with their nearest s_b spin from C . The scenario includes cases when $s_b \leq s_\ell$ as well as when $s_b > s_\ell$. Further, we consider bilinear-biquadratic interactions both for inter-spin interaction in C and also for the coupling between C and A (or B) except when $s_\ell = \frac{1}{2}$. The BBQ model of spin-1 chain (Eq. (2) with $J_2 = 0$), is known to host a variety of quantum phases including Haldane phases on a periodic chain [24, 49–53]. However, LDE properties on an open chain may not depend on the QPT points present in a periodic lattice [12].

Here also, we study entanglement between A and B as a function of coupling strength λ for different choices of BBQ parameter, θ corresponding to different quantum phases for the spin-1 chain (phases are known for the periodic boundary condition). We find that $\mathcal{E}^{\max} \sim 1$ for $\theta < 0$ irrespective of s_ℓ although both λ^m and \mathcal{E}^{\max} slightly decrease with s_ℓ (see Fig. 6) while for $\theta > 0$, the entanglement between A and B is very small and is highly dependent on system-size even at a low temperature like $\beta = 10^4$.

Firstly, we observe that the system-size dependence of \mathcal{E}^{\max} is much weaker for $s_b = 1$ than $s_b = \frac{1}{2}$, indicating a possibility for quasi-long-range entanglement over a longer distance with spin- $s_b (> \frac{1}{2})$ bulk. Secondly, for spin-1 bulk, the decay of entanglement \mathcal{E} in link sites with λ is much

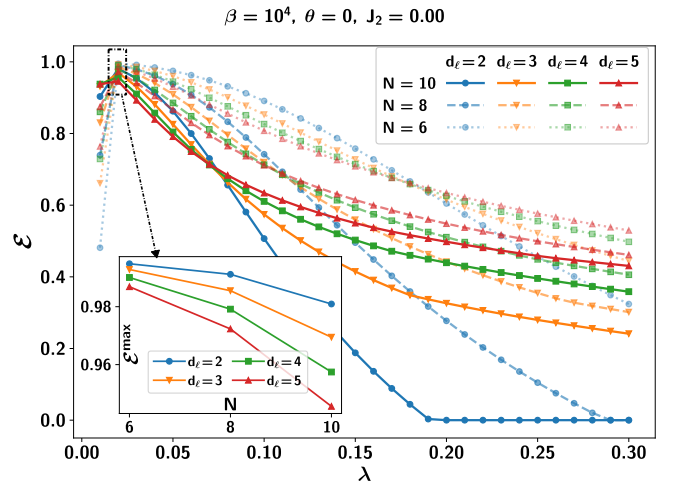


FIG. 7. \mathcal{E} (ordinate) as a function of the coupling strength λ (abscissa) for the spin-1 bulk. The interacting Hamiltonian in this case is chosen to be the Heisenberg interaction, i.e., $\theta = 0$ at very low temperature $\beta = 10^4$. All other specifications are same as in Fig. 6. Comparing with Fig. 6, we can realize that bilinear-biquadratic interactions can create more stable maximally entangled quantum link in terms of tuning of λ than that obtained via Heisenberg model. All quantities are dimensionless.

slower than that of the spin- $\frac{1}{2}$ bulk, thereby showing the advantage of the spin-1 bulk state. Specifically, the survival of near-maximum entanglement, i.e., $\mathcal{E} \approx 1$ occurs for a larger range of values of λ than the one observed for spin-1/2 bulk (comparing Figs. 3 and 6). It implies that the precise control of coupling between quantum link sites and the bulk is not required in this case which clearly establishes the *dimensional advantage*, especially from the point of view of realization. Note further that \mathcal{E}^{\max} exhibits stronger dependence on λ for Heisenberg-type inter-spin interaction ($\theta = 0$, see Fig. 7) among s_b spins since it again decreases faster from its maximum as λ is increased from λ^m compared to the case with $\theta < 0$ (comparing Figs. 6) and 7). This indicates a clear advantage of using both a spin-1 bulk C and bilinear-biquadratic interaction for obtaining maximal entanglement between two distant links having no direct interaction.

Temperature and NNN dependence of entanglement. Although in the case of spin- $\frac{1}{2}$ and spin-1 bulks, the maximal entanglement can be achieved between the links having arbitrary dimensions, we notice that the deviation from the maximal entanglement with the variation of temperature is substantial in the case of spin- $\frac{1}{2}$ bulk compared to the spin-1 bulk (comparing Fig. 8 with Fig. 4). However, \mathcal{E}^{\max} remains unaltered with the increase of J_2 and so in both the situations having spin $s_b (s_b = \frac{1}{2}, 1)$ bulk, \mathcal{E}^{\max} , λ^m , and $\mathcal{P}(\lambda^m)$ does not change with NNN interactions, thereby suggesting almost no role of NNN towards preparing the maximally entangled links (as shown in Figs. 4 and 8). More precisely, while the effect of J_2 is negligible for a very low temperature ($\beta \sim 10^4$ and higher), at a higher temperature ($\beta \sim 10^3$), small NNN interaction is found to slightly suppress the entanglement between A and B for $s_\ell = \frac{1}{2}$ while it mildly boosts entanglement

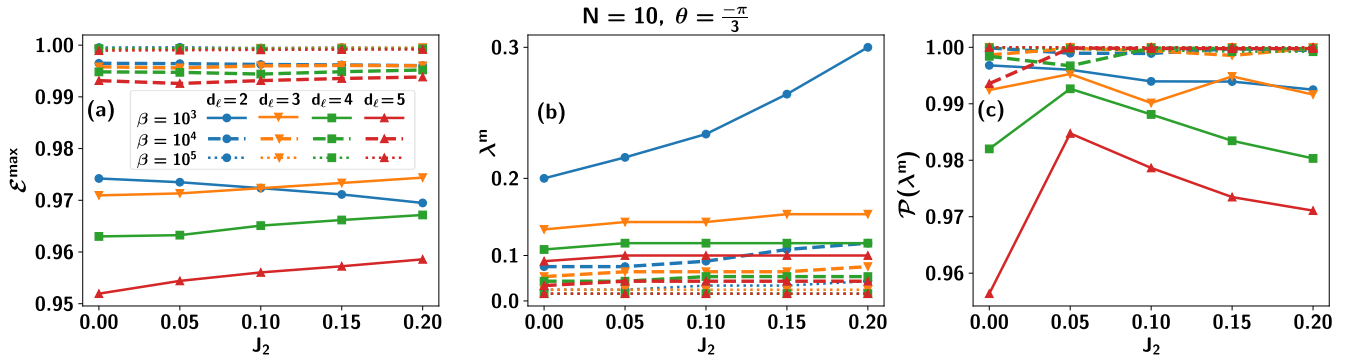


FIG. 8. (a) \mathcal{E}^{\max} with the variation of the NNN interaction strength J_2 (abscissa) for different values of the inverse temperature β in the spin-1 bulk. (b) The link interaction strength λ^m corresponding to \mathcal{E}^{\max} (ordinate), and (c) purity, $\mathcal{P}(\lambda^m)$ (ordinate) at λ^m . The system-size is $N = 10$. All the specifications in this figure is similar to the one considered for the spin-1/2 bulk in Fig. 4. All the quantities are dimensionless.

for higher s_ℓ . Further, NNN pushes λ^m upward for $s_\ell = \frac{1}{2}$ while λ^m for higher s_ℓ is mostly unaffected by the strength of J_2 . In this sense, it may indicate that having long-range interaction may be beneficial for the preparation of entanglement between two distant qudits whereas short-range interaction is more suitable for entangling two distant qubits at a moderate temperature.

IV. PROPOSAL TO CREATE AN ENTANGLED QUANTUM LINK IN DYNAMICS

In order to get highly entangled quantum link in the equilibrium, we showed in the preceding section that extremely low temperatures are required, which are typically hard to achieve in experiments. Moreover, keeping the system in equilibrium is not an easy enterprise. Therefore, it is appealing to determine a situation where after evolving the system by an interacting Hamiltonian, a highly entangled quantum link can be created from the appropriate product initial state. Precisely, the bulk is prepared as a completely polarised state which can be obtained at low temperature in the presence of a high magnetic field. Without any preferred direction of the $SU(2)$ symmetric Hamiltonian, we choose the initial state of the bulk as $|\Psi\rangle_C = \bigotimes_{i=2}^{N-1} |0\rangle_i$ (representing $\{|0\rangle, |1\rangle, \dots, |2s_b\rangle\}$ as the S^z -eigenbasis, with $|0\rangle$ corresponding to the maximum eigenvalue). Since such $|\Psi\rangle_C$ is an eigenstate of the $SU(2)$ symmetric bulk Hamiltonian H_b with zero entanglement (both bipartite as well as multipartite entanglement), this ensures that the entanglement generated between the quantum links are purely through interactions with the bulk. The links A and B are taken as pure states and oriented with the bulk in various directions. Hence the initial state can be written as

$$|\Psi^{\omega, \phi}(t=0)\rangle = |\psi_\ell^{\omega, \phi}\rangle_A \otimes \left(\bigotimes_{i=2}^{N-1} |0\rangle_i \right) \otimes |\psi_\ell^{\omega, \phi}\rangle_B, \quad (5)$$

with $|\psi_\ell^{\omega, \phi}\rangle = \hat{U}^z(\phi) \hat{U}^y(\omega) |\psi_\ell\rangle$, and $\hat{U}^\alpha(\delta) = \exp(-i\delta \hat{S}^\alpha)$ is the unitary rotation operator along α -axis by an angle δ . $|\psi_\ell\rangle$

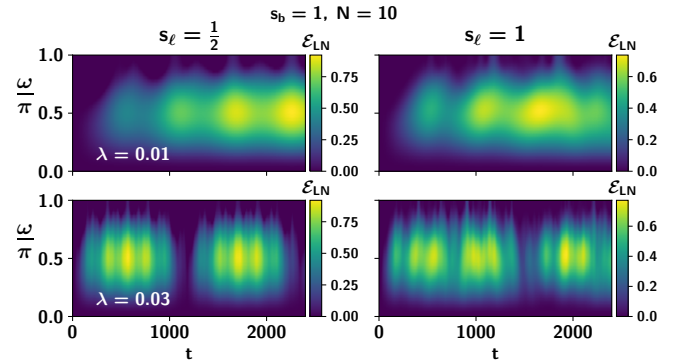


FIG. 9. Map plot of \mathcal{E} with the variation of t (horizontal axis) and $\frac{\omega}{\pi}$ (vertical axis). Note that ω/π rotation helps to create the suitable initial state in the link. The upper panels are for $\lambda = 0.01$ while the lower panels are for $\lambda = 0.03$. The initial state of the bulk is taken to be $|0\rangle^{\otimes N-2}$ and $s_b = 1$, and the quantum links are also taken as $|\psi_\ell\rangle^{s_\ell} = |0\rangle$. In the left column, $s_\ell = 1/2$ and in the right one, $s_\ell = 1$. The plots clearly depict that the entanglement of the link oscillates with time and a highly entangled quantum link can be produced over time, irrespective of the dimension of the link site. All the quantities are dimensionless.

is the link state which is rotated by ω and ϕ describing the relative rotation of the links in the y -direction, followed by z -rotation with respect to the bulk, resulting to the initial link state $|\psi_\ell^{\omega, \phi}\rangle_i$ ($i = A, B$). For example, taking $|\psi_\ell\rangle = |0\rangle$, the link site becomes $|\psi_\ell^{\omega, \phi}\rangle_{s_\ell=1/2} = \cos \frac{\omega}{2} |0\rangle + e^{i\phi} \sin \frac{\omega}{2} |1\rangle$, while in the case of spin-1, it takes the form as $|\psi_\ell^{\omega, \phi}\rangle_{s_\ell=1} = e^{-i\phi} \cos^2 \frac{\omega}{2} |0\rangle + \sqrt{2} \cos \frac{\omega}{2} \sin \frac{\omega}{2} |1\rangle + e^{i\phi} \sin^2 \frac{\omega}{2} |2\rangle$. Note that for arbitrary spin- s_ℓ , $|\psi^{s_\ell}(\omega, \phi)\rangle$ possesses a non-trivial form, which can be found. While for spin-1/2, (ω, ϕ) rotations on a single state access the complete local Hilbert space, this is not true for higher spin quantum numbers. For example, $\hat{U}^z(\phi) \hat{U}^y(\omega) |0\rangle \neq |1\rangle$, for any (ω, ϕ) with $s_\ell > \frac{1}{2}$. Preparation of these states require higher powers of the spin operators as local operators. Although in the case of spin-1/2, we can optimize over ω , and ϕ to obtain the initial link state, it is not

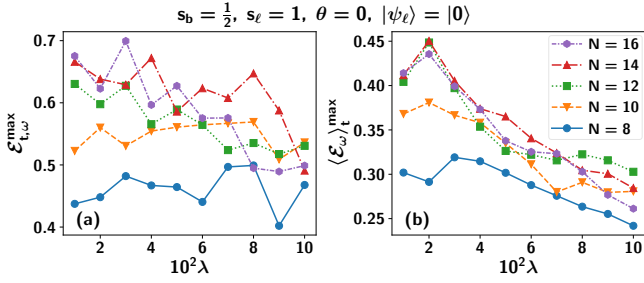


FIG. 10. (a) $\mathcal{E}_{t,\omega}^{\max}$ (ordinate) and (b) $\langle \mathcal{E}_{\omega} \rangle_t^{\max}$ against $10^2 \lambda$ (abscissa) for different values of the system-size. $\mathcal{E}_{t,\omega}^{\max}$ is obtained after maximizing over time, t and over ω involved in the rotation provided the initial state of the link is chosen to be $|\psi_\ell\rangle = |0\rangle$. The bulk is chosen to be $|0\rangle^{N-2}$ in all the calculations in dynamics, irrespective of the spin quantum number. Here $s_b = 1/2$. The evolving Hamiltonian is the Heisenberg model with $\theta = 0$. In the case of computing $\langle \mathcal{E}_{\omega} \rangle_t^{\max}$, we perform maximization over ω and the averaging is performed over time, t . Diamonds, triangle, squares, inverted triangle, and circles represent $N = 16, 14, 12, 10$ and 8 respectively. All the quantities are dimensionless.

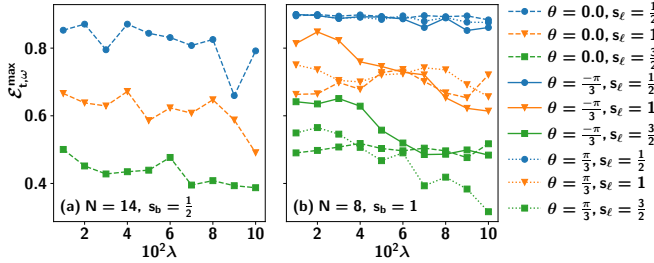


FIG. 11. $\mathcal{E}_{t,\omega}^{\max}$ (ordinate) against $10^2 \lambda$ (abscissa) for different values of the system-size and the bulk spin quantum number, namely (a) $N = 14, s_b = 1/2$ and (b) $N = 8, s_b = 1/2$. All other specifications are same as in Fig. 10. The system evolves according to the bilinear-biquadratic Hamiltonian with $\theta = 0$ (dashed line), $\theta = -\pi/3$ (solid line) and $\theta = \pi/3$ (dotted line). Circles, inverted triangles, squares are for $s_\ell = 1/2, 1$ and $3/2$ respectively. All the quantities are dimensionless.

the case for higher dimensional systems. Indeed, we observe that optimization over ω , and ϕ provides the initial state which leads to a highly entangled quantum link, although starting from $|1\rangle$ or $\frac{1}{\sqrt{d}} \sum_{i=0}^{d-1} |i\rangle$ in the link also produces a highly entangled state after adjusting system parameters properly.

The initial state, prepared as in Eq. (5), is evolved under the unitary evolution generated by the $SU(2)$ Hamiltonian as $|\Psi^{\omega,\phi}(t)\rangle = e^{-iH^{(s_\ell, s_b)} t} |\Psi^{\omega,\phi}(0)\rangle$. We observe that the entanglement in the resulting time-evolved state, $|\Psi^{\omega,\phi}(t)\rangle$, is invariant under the rotation along the axis of the bulk, i.e., with our choice of $|\Psi\rangle_C$ only $\hat{U}^y(\omega)$ creates a non-trivial entanglement dynamics, which reduces the parameter space. Note that without any relative rotation, i.e., $\omega=0, \phi=0$, the initial state is in the highest energy (ferromagnetically ordered) eigenstate of the evolving $SU(2)$ symmetric antiferromagnetic model, resulting in trivial dynamics and entanglement cannot be generated between the links.

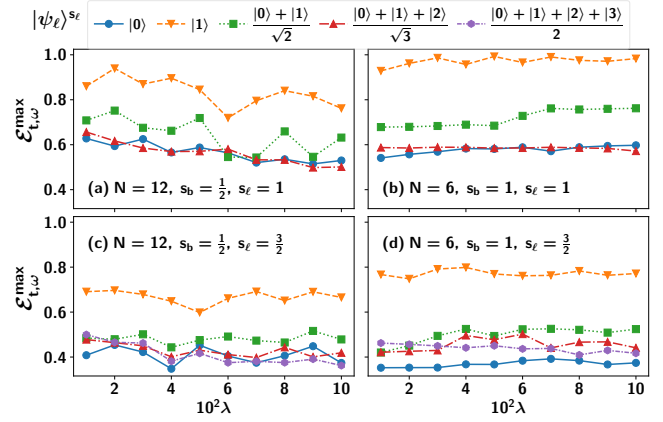


FIG. 12. **Role of initial state in the link.** $\mathcal{E}_{t,\omega}^{\max}$ (ordinate) vs $10^2 \lambda$ for different $|\psi_\ell\rangle$ as mentioned in the legends. Different plots represent different system-sizes and (s_ℓ, s_b) -pairs. Clearly, there exists initial link state $|1\rangle$ and λ values in the evolution operator which leads to a creation of maximally entangled quantum link (see (a) and (b)). All the quantities are dimensionless.

Let us first study the dynamics with $|\psi_\ell\rangle^{s_\ell} = |0\rangle$ for various (s_ℓ, s_b) pair. With the initial state as in Eq. (5), the dynamical state $|\Psi^{\omega,\phi}(t)\rangle$ gets the quantum links entangled with entanglement increasing initially with time t . Fig. 9 illustrates the entanglement dynamics, when the evolution is generated by the Heisenberg Hamiltonian ($\theta = 0$) with the spin-1 bulk. After oscillations, the quantum links becomes disentangled again in the time scale $\propto \lambda^{-1}$ and then entangled again. We also observe that the maximum amount of entanglement is generated between the links, when they are $\sim \pi/2$ rotated. The time scale of oscillations are observed to be increasing with system-size N which leads to a finite-size study. We compute the maximum entanglement generated $\mathcal{E}_{t,\omega}^{\max}$ and average entanglement generated over time $\langle \mathcal{E}_{\omega} \rangle_t^{\max}$. Interestingly, both the quantities increase with system-size, shown for $|\psi_\ell\rangle = |0\rangle$ with $s_b = 1/2$ and $s_\ell = 1$ in Fig. 10. For this (s_ℓ, s_b) pair, the both $\mathcal{E}_{t,\omega}^{\max}$ and $\langle \mathcal{E}_{\omega} \rangle_t^{\max}$ saturate for $N = 14$, with $\mathcal{E}_{t,\omega}^{\max} \sim 0.7$ for the spin-1 links.

Let us compare the entanglement created in links for different bulk spins s_b , along with different BBQ parameter θ . First, with only Heisenberg interactions, we find that the maximum entanglement $\mathcal{E}_{t,\omega}^{\max}$ between the quantum links decreases with increasing link spin quantum number s_ℓ (Fig. 11), i.e., with $s_b = 1/2$ ($N = 14$), $\mathcal{E}_{t,\omega}^{\max} \sim 0.8, 0.6, 0.4$ for $s_\ell = 1/2, 1$ and $3/2$ respectively whereas the $s_b = 1$ ($N = 8$) bulk chain can create more entangled quantum links than the $s_b = 1/2$ one, with $\mathcal{E}_{t,\omega}^{\max} \sim 0.9, 0.7, 0.5$ for $s_\ell = 1/2, 1$ and $3/2$ respectively, revealing the benefit of the local spin dimension of the bulk. The situation can further be improved for $s_b = 1$ bulk spins, with the BBQ parameter θ . While the $\mathcal{E}_{t,\omega}^{\max}$ remains similar for $\theta = \pi/3$, the situation is different for $\theta = -\pi/3$. The quantum links can be further entangled, with $\mathcal{E}_{t,\omega}^{\max}$ reaching ~ 0.8 and 0.65 , from 0.7 and 0.5 for $s_\ell = 1$ and $s_\ell = 3/2$ respectively. This further enhances the entanglement between the quantum links of higher spin quantum numbers. More

importantly, notice that in the equilibrium situation, the BBQ model $\theta > 0$ cannot produce entangled quantum link although it can be generated through dynamics.

In the case of $s_\ell > 1/2$, the local Hilbert space is not completely spanned by the unitary rotations on $|\psi_\ell\rangle^{s_\ell} = |0\rangle$, for $\mathcal{E}_{t,\omega}^{\max}$. For $s_\ell = 1$, and $3/2$, we take different starting quantum link states, $|\psi_\ell\rangle^{s_\ell}$ as shown in Fig. 12. Interestingly, the quantum links are highly entangled, when the quantum links are initialized as $|\psi_\ell\rangle^{s_\ell} = |1\rangle$, with $\mathcal{E}_{t,\omega}^{\max} \sim 1$ for $s_b = s_\ell = 1$, i.e., maximally entangled two-qutrit state can be created even for a small system size, $N = 6$. This possibly indicates that the situation could even be improved if one maximizes over all possible initial states of the quantum link, and the BBQ Hamiltonian can be used to dynamically create highly entangled quantum links.

V. CONCLUSION

Creating long-distance entangled quantum link can be a crucial component of quantum communication and for the scalability of quantum computer. On the other hand, instead of two-qubit entangled states, sharing higher dimensional entangled states has been demonstrated to be beneficial for several quantum information tasks including quantum cryptography, quantum computation etc.

This work addresses the problem of sharing long-distance highly entangled states in arbitrary dimensions between two distant locations that are weakly coupled with a large number of interacting spins, referred to as a processor or a bulk. In an equilibrium scenario, we found that creating a two-qudit maximally entangled state occurs when the bulk consists of interacting spin-1/2 or spin-1 systems in which the interactions are governed by either nearest-neighbor Heisenberg Hamiltonian or bilinear-biquadratic Heisenberg model with spin- s ($s > 1/2$). However, when the bulk state is spin-1, the maximum entanglement is shown to be more stable towards adjust-

ing the system parameters compared to the spin-1/2 bulk including the temperature of the system. Moreover, we observed that the two-qudit maximally entangled quantum link remains so even when the next nearest-neighbor interactions are incorporated in the system provided the temperature is very low. We analyzed the spin- s Hamiltonian by diagonalizing it using the Lanczos approach and selecting the lowest energy eigenstates.

Preparing the system at a very low temperature and retaining it in equilibrium, hence preserving the maximally entangled state over a long distance, is a challenging endeavor. Hence we go beyond the equilibrium situation and dynamically prepare the entangled quantum link. In particular, the initial state is prepared as a completely polarized product state in the bulk and the quantum link is formed by rotating the completely polarized state at a specific angle. The system undergoes an evolution according to the Heisenberg and bilinear-biquadratic Hamiltonian, resulting in the creation of a highly entangled quantum link. Unlike the equilibrium situation, the produced highly entangled quantum link over time depends on the system-size of the bulk and grows favorably as the system-size increases.

VI. ACKNOWLEDGEMENTS

We acknowledge the support from the Interdisciplinary Cyber Physical Systems (ICPS) program of the Department of Science and Technology (DST), India, Grant No.: DST/ICPS/QuST/Theme- 1/2019/23 and TARE Grant No.: TAR/2021/000136. We acknowledge the use of QIClib – a modern C++ library for general-purpose quantum information processing and quantum computing (<https://titaschanda.github.io/QIClib>) and high-performance computing facility at Harish-Chandra Research Institute.

-
- [1] R. Horodecki, P. Horodecki, M. Horodecki, and K. Horodecki, *Rev. Mod. Phys.* **81**, 865 (2009).
 - [2] E. Schrödinger, *Mathematical Proceedings of the Cambridge Philosophical Society* **31**, 555563 (1935).
 - [3] I. L. C. Michael A. Nielsen, *Quantum Information and Quantum Computation*.
 - [4] J.-W. Pan, Z.-B. Chen, C.-Y. Lu, H. Weinfurter, A. Zeilinger, and M. Żukowski, *Rev. Mod. Phys.* **84**, 777 (2012).
 - [5] J. I. Cirac, A. K. Ekert, S. F. Huelga, and C. Macchiavello, *Phys. Rev. A* **59**, 4249 (1999).
 - [6] H.-J. Briegel, W. Dür, J. I. Cirac, and P. Zoller, *Phys. Rev. Lett.* **81**, 5932 (1998).
 - [7] W. Dür, H.-J. Briegel, J. I. Cirac, and P. Zoller, *Phys. Rev. A* **59**, 169 (1999).
 - [8] D. Kielpinski, C. Monroe, and D. J. Wineland, *Nature* **417**, 709 (2002).
 - [9] B. B. Blinov, D. L. Moehring, L.-M. Duan, and C. Monroe, *Nature* **428**, 153 (2004).
 - [10] A. J. Skinner, M. E. Davenport, and B. E. Kane, *Phys. Rev. Lett.* **90**, 087901 (2003).
 - [11] S. Bose, *Contemporary Physics* **48**, 13 (2007), <https://doi.org/10.1080/00107510701342313>.
 - [12] L. Campos Venuti, C. Degli Esposti Boschi, and M. Roncaglia, *Phys. Rev. Lett.* **96**, 247206 (2006).
 - [13] A. Wójcik, T. Łuczak, P. Kurzyński, A. Grudka, T. Gdala, and M. Bednarska, *Phys. Rev. A* **72**, 034303 (2005).
 - [14] L. Campos Venuti, S. M. Giampaolo, F. Illuminati, and P. Zanardi, *Phys. Rev. A* **76**, 052328 (2007).
 - [15] S. M. Giampaolo and F. Illuminati, *New Journal of Physics* **12**, 025019 (2010).
 - [16] N. Y. Yao, L. Jiang, A. V. Gorshkov, Z.-X. Gong, A. Zhai, L.-M. Duan, and M. D. Lukin, *Phys. Rev. Lett.* **106**, 040505 (2011).
 - [17] T. J. G. Apollaro, L. Banchi, A. Cuccoli, R. Vaia, and P. Verrucchi, *Phys. Rev. A* **85**, 052319 (2012).
 - [18] H. S. Dhar, D. Rakshit, A. Sen(De), and U. Sen, *Europhysics Letters* **114**, 60007 (2016).

- [19] V. Coffman, J. Kundu, and W. K. Wootters, *Phys. Rev. A* **61**, 052306 (2000).
- [20] L. Campos Venuti, C. Degli Esposti Boschi, and M. Roncaglia, *Phys. Rev. Lett.* **99**, 060401 (2007).
- [21] L. Hu, Y. Xu, P. Zhang, S. Yan, and X. Kong, *Physica A: Statistical Mechanics and its Applications* **607**, 128170 (2022).
- [22] A. Ferreira and J. M. B. L. dos Santos, *Phys. Rev. A* **77**, 034301 (2008).
- [23] L. C. Venuti and M. Roncaglia, *Phys. Rev. Lett.* **94**, 207207 (2005).
- [24] M. V. Rakov and M. Weyrauch, *Phys. Rev. B* **105**, 024424 (2022).
- [25] S. Sahling, G. Remenyi, C. Paulsen, P. Monceau, V. Saligrama, C. Marin, A. Revcolevschi, L. P. Regnault, S. Raymond, and J. E. Lorenzo, *Nature Physics* **11**, 255 (2015).
- [26] N. Y. Yao, L. Jiang, A. V. Gorshkov, P. C. Maurer, G. Giedke, J. I. Cirac, and M. D. Lukin, *Nature Communications* **3**, 800 (2012).
- [27] N. Gisin and A. Peres, *Phys. Lett. A* **162**, 15 (1992).
- [28] D. Collins, N. Gisin, N. Linden, S. Massar, and S. Popescu, *Phys. Rev. Lett.* **88**, 040404 (2002).
- [29] W. Son, J. Lee, and M. S. Kim, *Phys. Rev. Lett.* **96**, 060406 (2006).
- [30] N. J. Cerf, M. Bourennane, A. Karlsson, and N. Gisin, *Phys. Rev. Lett.* **88**, 127902 (2002).
- [31] T. Durt, N. J. Cerf, N. Gisin, and M. Żukowski, *Phys. Rev. A* **67**, 012311 (2003).
- [32] D. Cozzolino, B. Da Lio, D. Bacco, and L. K. Oxenlwe, *Advanced Quantum Technologies* **2**, 1900038 (2019).
- [33] T. C. Ralph, K. J. Resch, and A. Gilchrist, *Phys. Rev. A* **75**, 022313 (2007).
- [34] J. Wang, Y. Lai, Z. Ye, J. He, Y. Ma, and Q. Liao, *Phys. Rev. E* **91**, 050102 (2015).
- [35] F.-Q. Dou, Y.-J. Wang, and J.-A. Sun, *EPL (Europhysics Letters)* **131**, 43001 (2020).
- [36] A. C. Santos, B. i. e. i. f. m. c. Çakmak, S. Campbell, and N. T. Zinner, *Phys. Rev. E* **100**, 032107 (2019).
- [37] A. Usui, W. Niedenzu, and M. Huber, *Phys. Rev. A* **104**, 042224 (2021).
- [38] S. Ghosh and A. Sen(De), *Phys. Rev. A* **105**, 022628 (2022).
- [39] T. K. Konar, S. Ghosh, A. K. Pal, and A. Sen(De), *Phys. Rev. A* **107**, 032602 (2023).
- [40] J. Joo, P. L. Knight, J. L. O'Brien, and T. Rudolph, *Phys. Rev. A* **76**, 052326 (2007).
- [41] E. Nagali, D. Giovannini, L. Marrucci, S. Slussarenko, E. Santamato, and F. Sciarrino, *Phys. Rev. Lett.* **105**, 073602 (2010).
- [42] F. Bouchard, R. Fickler, R. W. Boyd, and E. Karimi, *Science Advances* **3** (2017), 10.1126/sciadv.1601915.
- [43] F. Bouchard, K. Heshami, D. England, R. Fickler, R. W. Boyd, B.-G. Englert, L. L. Sanchez-Soto, and E. Karimi, *Quantum* **2**, 111 (2018).
- [44] P. Imany, J. A. Jaramillo-Villegas, M. S. Alshaykh, J. M. Lukens, O. D. Odele, A. J. Moore, D. E. Leaird, M. Qi, and A. M. Weiner, *npj Quantum Information* **5**, 59 (2019).
- [45] M. Erhard, R. Fickler, M. Krenn, and A. Zeilinger, *Light: Science & Applications* **7**, 17146 (2018).
- [46] P. J. Low, B. M. White, A. A. Cox, M. L. Day, and C. Senko, *Phys. Rev. Research* **2**, 033128 (2020).
- [47] V. A. Soltamov, C. Kasper, A. V. Poshakinskiy, A. N. Anisimov, E. N. Mokhov, A. Sperlich, S. A. Tarasenko, P. G. Baranov, G. V. Astakhov, and V. Dyakonov, *Nature Communications* **10**, 1678 (2019).
- [48] M. Neeley, M. Ansmann, R. C. Bialczak, M. Hofheinz, E. Lucero, A. D. O'Connell, D. Sank, H. Wang, J. Wenner, A. N. Cleland, M. R. Geller, and J. M. Martinis, *Science* **325**, 722 (2009).
- [49] C. K. Lai, *Journal of Mathematical Physics* **15**, 1675 (1974).
- [50] B. Sutherland, *Phys. Rev. B* **12**, 3795 (1975).
- [51] H. Babujian, *Physics Letters A* **90**, 479 (1982).
- [52] G. Fáth and J. Sólyom, *Phys. Rev. B* **44**, 11836 (1991).
- [53] G. Fáth and J. Sólyom, *Phys. Rev. B* **47**, 872 (1993).
- [54] G. Vidal and R. F. Werner, *Phys. Rev. A* **65**, 032314 (2002).
- [55] A. Peres, *Phys. Rev. Lett.* **77**, 1413 (1996).
- [56] M. Horodecki, P. Horodecki, and R. Horodecki, *Physics Letters A* **223**, 1 (1996).
- [57] M. Horodecki, P. Horodecki, and R. Horodecki, *Phys. Rev. Lett.* **80**, 5239 (1998).
- [58] D. P. DiVincenzo, P. W. Shor, J. A. Smolin, B. M. Terhal, and A. V. Thapliyal, *Phys. Rev. A* **61**, 062312 (2000).
- [59] W. Dür, J. I. Cirac, M. Lewenstein, and D. Bruß, *Phys. Rev. A* **61**, 062313 (2000).
- [60] H.-P. Breuer, *Journal of Physics A: Mathematical and General* **38**, 9019 (2005).
- [61] C. Lanczos, *Journal of Research of the National Bureau of Standards* **45**, 255 (1950).
- [62] C. Sanderson and R. Curtin, *Journal of Open Source Software* **1**, 26 (2016).
- [63] C. Sanderson and R. Curtin, *Mathematical and Computational Applications* **24** (2019), 10.3390/mca24030070.
- [64] A. Weiße, G. Wellein, A. Alvermann, and H. Fehske, *Rev. Mod. Phys.* **78**, 275 (2006).
- [65] P. Sierant, K. Biedro, G. Morigi, and J. Zakrzewski, *SciPost Phys.* **7**, 008 (2019), appendix C.
- [66] J. Schachenmayer, B. P. Lanyon, C. F. Roos, and A. J. Daley, *Phys. Rev. X* **3**, 031015 (2013).
- [67] A. S. Buyskikh, M. Fagotti, J. Schachenmayer, F. Essler, and A. J. Daley, *Phys. Rev. A* **93**, 053620 (2016).
- [68] I. Frérot, P. Naldesi, and T. Roscilde, *Phys. Rev. B* **95**, 245111 (2017).
- [69] L. G. C. Lakkaraju, S. Ghosh, S. Roy, and A. Sen(De), *Physics Letters A* **418**, 127703 (2021).
- [70] H. Tasaki, "Basics of quantum spin systems," in *Physics and Mathematics of Quantum Many-Body Systems* (Springer International Publishing, Cham, 2020) pp. 13–45.